Title

Influence of agricultural managed aquifer recharge on nitrate transport: The role of soil texture and flooding frequency

Journal

Vadose Zone Journal, 20(5)

ISSN

1539-1663

Authors

Murphy, Nicholas P
Waterhouse, Hannah
Dahlke, Helen E

Publication Date

2021-09-01

DOI

10.1002/vzj2.20150

Peer reviewed

Received: 6 May 2021 | Accepted: 9 June 2021

DOI: 10.1002/vzj2.20150

Vadose Zone Journal

ORIGINAL RESEARCH ARTICLE

Influence of agricultural managed aquifer recharge on nitrate transport: The role of soil texture and flooding frequency

Nicholas P. Murphy | **Hannah Waterhouse** | **Helen E. Dahlke**

Dep. of Land, Air and Water Resources, Univ. of California, Davis, CA 95616, USA

Correspondence
Nicholas P. Murphy, Dep. of Land, Air and Water Resources, Univ. of California, Davis, CA 95616, USA.
Email: npmurphy@ucdavis.edu

Assigned to Associate Editor Kenton Rod.

Funding information
National Institute of Food and Agriculture, Grant/Award Number: CA-D-LAW-2513-H; Almond Board of California; Bureau of Reclamation, Grant/Award Number: R16PC00029

Abstract

Agricultural managed aquifer recharge (Ag-MAR) is a concept in which farmland is flooded during the winter using excess surface water to recharge the underlying groundwater. In this study, we show how different recharge practices affect NO_3^- leaching and mineralization–denitrification processes in different soil systems. Two contrasting soil textures (sand and fine sandy loam) from the Central Valley, California, were repeatedly flooded with 15 cm of water at varying time intervals in field and soil column experiments. Nitrogen species (NO_3^-, NH_4^+, total N), total C, dissolved O_2, and moisture content were measured throughout the experiments. Results show that when flooding occurs at longer intervals (every 1–2 wk), N mineralization increases, leading to an increase of mobile NO_3^- in the upper root zone and leaching of significant quantities of NO_3^- from both soil textures (137.3 ± 6.6% [sand] and 145.7 ± 5.8% [fine sandy loam] of initial residual soil NO_3^-) during subsequent flooding events. Laboratory mineralization incubations show that long flooding intervals promote mineralization and production of excess NO_3^- at rates of 0.11–3.93 mg N kg^{-1} wk^{-1} (sand) and 0.08–3.41 mg N kg^{-1} wk^{-1} (fine sandy loam). Decreasing the flooding frequency to 72 h reduces potential mineralization, decreasing the amount of NO_3^- leached during flooding events (31.7 ± 3.8% [sand] and 64.7 ± 10.4% [fine sandy loam] of initial residual soil NO_3^-). The results indicate that implementing recharge as repeated events over a long (multiple-week) time horizon might increase the total amount of NO_3^- potentially available for leaching to groundwater.

1 | INTRODUCTION

Dependence on groundwater for irrigation and consumptive use has resulted in the widespread depletion of groundwater aquifers across the world (Dalin et al., 2019; Wada et al., 2014). In most of the semiarid U.S. Southwest, groundwater is increasingly being regulated in efforts to sustainably manage this limited resource. Sustainably managing groundwater in California has increased the interest in and use of managed aquifer recharge (MAR) technologies that purposefully recharge water to aquifers for subsequent recovery or environmental benefit (Dillon et al., 2009).

Agricultural managed aquifer recharge (Ag-MAR) is a promising form of managed aquifer recharge, where farmland is flooded during the winter using excess surface water in

Abbreviations: Ag-MAR, agricultural managed aquifer recharge; HF, high-frequency flooding; LF, low-frequency flooding; MAR, managed aquifer recharge; TC, total carbon; TN, total nitrogen; VWC, volumetric soil water content; WA, water application.

order to recharge the underlying groundwater aquifer (Kocis & Dahlke, 2017). Over 3.6 million ha of suitable farmland that is connected to water conveyance systems has been identified for Ag-MAR throughout the Central Valley of California (O'Geen et al., 2015). Some of these lands support infiltration rates in excess of 50 cm d^{-1}, raising questions on how Ag-MAR could be implemented on suitable but fertilized agricultural fields such that NO_3^- leaching from the root zone to the groundwater is minimized.

The risk of NO_3^- leaching to the underlying groundwater stems from N accumulation in the soil profile as a result of repeated fertilizer applications and incomplete N uptake by crops (Di & Cameron, 2002b). Overapplication of N fertilizer has been reported as a major contributing factor to the accumulation of NO_3^- in the soil profile (0–400 cm) as shown by Zhou et al. (2016), who observed a residual NO_3^- load of 453–2,155 kg N ha^{-1} in the North China Plain and Loess Plateau, China. Harter et al. (2005) observed the accumulation of 218–477 kg N ha^{-1} in the deep vadose zone (1,600-cm depth) under a citrus (*Citrus* L. spp.) orchard in California. These residual NO_3^- loads in the root zone or deep vadose zone are at risk of being leached when large amounts of water (e.g. >10–15 cm d^{-1}) are applied for Ag-MAR, which could potentially lead to water quality degradation of underlying groundwater resources (Botros et al., 2012; Onsoy et al., 2005).

Research regarding NO_3^- transport in the vadose zone has been conducted in agricultural settings under various irrigation practices, such as drip (Baram et al., 2016; Lv et al., 2019; Phogat et al., 2014), sprinkler (Baram et al., 2016; Gheysari et al., 2009), and flood irrigation (Di & Cameron, 2002a; Wang et al., 2010). These studies have concluded that N supply from the vadose zone to the groundwater is transport limited rather than source limited, with the most efficient irrigation systems (drip and sprinkler) leaching lower amounts of NO_3^- from the soil profile. Drip irrigation paired with optimized N fertilization has been shown to reduce NO_3^- leaching by 90% compared with conventional flood irrigation practices (Di & Cameron, 2002; Lv et al., 2019; Wang et al., 2010). Flood irrigation is an irrigation method similar to Ag-MAR, often with a smaller ponding depth and shorter application duration than is applied during Ag-MAR. As such, these studies provide insights into how larger water applications and ponded conditions might influence NO_3^- leaching. Wang et al. (2010) flooded a winter wheat (*Triticum aestivum* L.)–summer maize (*Zea mays* L.) cropping systems on a silt loam soil in the North China Plain every 72 h with two 25-cm water applications and found that 62 ± 7% of the NO_3^- within the upper 200 cm of the soil profile was leached. Lv et al. (2019) reported that flood irrigation of tomato (*Solanum lycopersicum* L.) fields in a silt loam at an agricultural experimental station in Tianjin City, China, showed low N use efficiency resulting in 50% of total N input being leached (300 kg N ha^{-1} per season). Hence, in many irrigated agricultural regions, precision irrigation and/or deficit irrigation are increasingly used to minimize NO_3^- leaching and to trap residual NO_3^- in or below the root zone (Baram et al., 2016; Gheysari et al., 2009; Waddell et al., 2000). Therefore, AgMAR represents a significant hydrologic regime shift from current growing season irrigation practices in semiarid climates.

Core Ideas

- Short-lived Ag-MAR flooding events cause NO_3^- leaching and organic N mineralization.
- Soil texture affects the timing of NO_3^- leaching under Ag-MAR.
- Soil texture affects the conditions for biogeochemical processes under Ag-MAR.
- Reducing time between flooding events for Ag-MAR reduces NO_3^- produced by mineralization.

To date, not many studies exist that have investigated the impact of Ag-MAR on NO_3^- leaching and N transformation processes in the root zone. Among the few studies that do exist, Bachand et al. (2014) concluded that although NO_3^- will initially be leached to the groundwater under Ag-MAR, there is the potential to improve groundwater quality over time through subsequent flooding applications with low-N water. Waterhouse et al. (2020) assessed the root zone residual NO_3^- load of farm fields representing different soil textures, crop types, and management practices to quantify the risk of groundwater contamination under Ag-MAR, concluding that wine grape (*Vitis vinifera* L.) vineyards on permeable soils had the lowest observed NO_3^- leaching risk. They noted that further research is needed regarding the relationship between NO_3^- leaching, Ag-MAR practices (e.g., frequency and duration of floodwater applications), and soil texture.

Soil texture has been shown to significantly affect both the hydrologic flow properties and conditions favorable to biogeochemical transformations. Soil texture affects infiltration rates and residence time of applied water and thus NO_3^- mobilization, potential sorption of N species, O_2 content, oxidation–reduction potential, and microbial activity, all factors that may affect biogeochemical processes (Aronsson & Bergström, 2001; Bergström & Johansson, 1991; Kaiser et al., 1992; Sogbedji et al., 2000). Gaines and Gaines (1994) examined the impact of soil texture and organic matter content on NO_3^- leaching potential and found that increased fractions of silt, clay, and organic matter in a soil decrease the amount of NO_3^- leaching observed. Mineralization of organic N, under favorable temperature (>25 °C) and moisture conditions (~55% water holding capacity), increases inorganic N concentrations within the soil profile, which are then

susceptible to leaching (Cabrera, 1993; Cambardella et al., 1999; Linn & Doran, 1984). Conversely, the transition from an oxic to an anoxic soil environment affects the potential for denitrification, which can decrease the NO_3^- leaching potential of a soil due to the transformation of NO_3^- to N_2 gas.

Nitrate leaching and N transformation processes have been studied in more detail in traditional MAR systems such as storm water or treated wastewater infiltration basins (Abiye et al., 2009; Ben Moshe et al., 2020; Goren et al., 2014; Gorski et al., 2019; Schmidt et al., 2011). Depending on the infiltration rate of the native soil, Schmidt et al. (2011) observed a 30–60% removal of NO_3^- in agricultural storm runoff recharged in a 3-ha infiltration basin. Soil aquifer treatment (SAT) systems, a special form of MAR aimed at infiltrating wastewater or reclaimed water, can result in dramatic water quality improvements by forcing soil systems towards favorable (e.g., anoxic) biogeochemical conditions. The physical and biochemical processes that occur during passage of the wastewater through the biologically active infiltration interface in the top meter of the infiltration basin sediments are key to N removal due to denitrification (Miller et al., 2006). Soil aquifer treatment research has further highlighted the utility of controlled soil column experiments in examining spatially and temporally complex soil conditions and their impact on biogeochemical transformations (Ben Moshe et al., 2020; Goren et al., 2014; Quanrud et al., 1996). However, traditional MAR and SAT systems are often focused on remediating NO_3^- loads or other contaminants from the infiltrating recharge water, as opposed to Ag-MAR where the NO_3^- leaching potential stems from the residual NO_3^- stored in the soil matrix or vadose zone.

Although traditional MAR systems have similar end goals to Ag-MAR, major hydrologic differences exist between these systems. In contrast with MAR infiltration basins, which often maintain a constant head of several meters for several weeks, creating a thick saturated layer beneath the basin surface (Gorski et al., 2019; Schmidt et al., 2011), previous Ag-MAR projects often had smaller heads (10–50 cm). In addition, on agricultural fields planted with perennial crops, the water was applied in short-lived pulses on high-infiltration-capacity soils to avoid waterlogged conditions that could potentially harm the crops. These pulsed water applications create more distinct wetting–drying cycles and dynamic changes in environmental conditions and biogeochemical processes than are found in continuously flooded systems (Dahlke et al., 2018). For these highly dynamic systems, not much is known about the effect that soil texture or Ag-MAR flooding frequency (how often water is applied for recharge) have on NO_3^- leaching potential.

The aim of this research is to quantify NO_3^- leaching and N transformation processes in the soil and shallow vadose zone of agricultural soils subject to different Ag-MAR practices. Our study specifically investigates the following questions:

1. What effect does soil texture have on NO_3^- leaching and N transformation processes during Ag-MAR?
2. What effect does varying flooding frequency have on NO_3^- leaching and N transformation processes during Ag-MAR?

We hypothesize that soil texture and flooding frequency are controlling factors on the amount of residual soil NO_3^- that is being leached from the root zone, since both parameters influence the wetting and drainage, O_2, and redox regime of the soil and with that the environmental conditions favoring specific N transformation processes such as denitrification or mineralization. Soil texture is hypothesized to be particularly influential on the amount of NO_3^- leached from the profile, with coarser textures allowing more leaching than finer textured soils. Flooding frequency is hypothesized to affect mineralization and denitrification potential in both soils, with higher flooding frequencies promoting environmental conditions more favorable for denitrification and less for mineralization. To evaluate the posed questions and hypotheses, we used data from field experiments at two almond [*Prunus dulcis* (Mill.) D.A. Webb] orchards in the Central Valley of California and laboratory soil column experiments, in which we tested the effects of flooding frequency and soil texture in a controlled environment. In addition, we completed incubation experiments to gain a mechanistic understanding of N transformation processes and rates for these soil textures.

2 | MATERIALS AND METHODS

2.1 | Field experiments

2.1.1 | Study sites

Two almond orchards were investigated during the winters of 2015–2016 and 2016–2017, both located in the Central Valley of California. The first site is located south of Delhi, CA (37°24′12″ N, 120°47′19″ W), whereas the second is located southwest of Modesto, CA (37°36′26″ N, 121° 4′21″ W) (Figure 1). The soil at Delhi is a sand (Delhi sand series; mixed, thermic, Typic Xeropsamments), a rapidly draining soil with high infiltration rates (average profile saturated hydraulic conductivity [K_{sat}] ~ 30 cm h^{-1}). The presence of a hardpan layer around 100-cm depth was previously observed at Delhi; however, deep ripping of the hardpan occurred prior to the original planting of the orchard in the early 2000s. The soil at Modesto is a fine sandy loam, a moderately draining soil derived from granitic alluvium (Dinuba series; coarse-loamy, mixed, active, thermic Typic Haploxeralfs; Soil Series USDA). Hereafter, the two field sites will be referenced to as sand (Delhi) and fine sandy loam (Modesto). The two sites are rated as "excellent" (sand) and "moderately good" (fine sandy

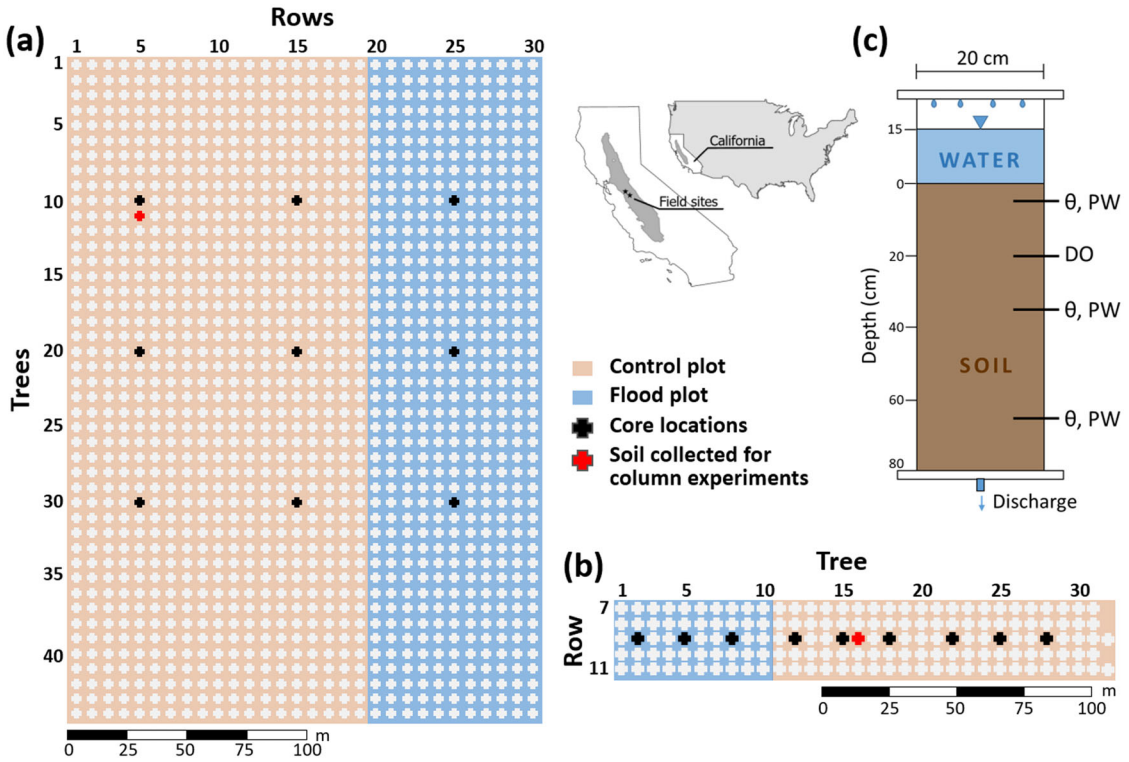

FIGURE 1 Study locations and experimental setup. (a) Fine sandy loam experimental field design; (b) sand experimental field design; and (c) experimental laboratory column design, where θ is volumetric water content sensor, PW is pore water sampler, and DO is dissolved O_2 sensor

loam) by the Soil Agricultural Groundwater Banking Index (SAGBI; O'Geen et al., 2015), a recently proposed measure of Ag-MAR soil suitability. The mean annual precipitation at both sites varied between 17.8 and 36.1 cm from 2015 to 2018: 2015 was a critical dry year, and 2017 was the second wettest year on the 100-yr climate record in California. The majority of precipitation at both sites occurs during the winter months (November–April), and the mean annual temperature is 17.25 ˚C (January 2015–2018) (Soil Series USDA, California Irrigation Management Information System [CIMIS] Station 206).

2.1.2 | Field instrumentation and monitoring

Two treatments were tested at each orchard: a flood treatment (i.e., Ag-MAR) in which 61 cm of water was applied during December–January (2015–2016 and 2016–2017) in three or four separate flooding events, with 15.24–25.4 cm of applied water during each event (supplemental material; Table 1), and the grower standard irrigation practices, defined as the control. The average NO_3^-–N concentration of the applied water was 9.63 mg L^{-1} for the sand field site, and 1.45 mg L^{-1} for the fine sandy loam field site. The variation in NO_3^- concentration of the applied water between sites is reflective of the water source that was used for flooding: the fine sandy loam site used local surface water, and the sand site used pumped groundwater in lieu of available surface water resources. Soil cores (5-cm diam.) were collected using a direct push drill method (Geoprobe Systems) before and after winter flooding events, to a depth of 300–400 cm.

Cores were analyzed for soil texture, NO_3^-–N, NH_4^+–N, total C (TC), and total N (TN). Soil samples were prepared for N analysis using 0.5 M K_2SO_4 extractions, whereby 15 g of soil (corrected for soil water content) was extracted with 36 ml K_2SO_4, with extracted supernatant representing soil extractable N. All NO_3^-–N and NH_4^+–N samples in both field and laboratory experiments were analyzed using the vanadium (III) reduction (Doane & Horwath, 2003) and the Berthelot reaction (Forster, 1995; Verdouw et al., 1978), respectively. The TC and TN soil samples were ball milled and analyzed using the Costech ECS 4010. Soil samples taken before and after recharge events were analyzed in triplicate samples for NO_3^-–N, NH_4^+–N, and TN, in 10-cm intervals, which allowed constraining both the organic N and inorganic N pools within the soil matrix.

2.2 | Laboratory experiments

2.2.1 | Soil column experiments

Laboratory soil column experiments were designed to corroborate data collected from field-scale experiments and to

TABLE 1 Sand and fine sandy loam field core NO_3^-–N loads. The root zone (RZ) is defined as the first 100 cm of the core, whereas "full" denotes the entire 400-cm profile or core length

Parameter	NO_3–N load before flood (RZ)	NO_3–N load after flood (RZ)	Change	NO_3–N load before flood (full profile)	NO_3–N load after flood (full profile)	Change
	kg ha^{-1}		%	kg ha^{-1}		%
	Sand (2015–2016)					
Flood avg. ($n = 3$)	44.12 ± 28.55	5.41 ± 0.65	−82 ± 15	286.03 ± 257.49	115.36 ± 54.39	−23 ± 85
Control avg. ($n = 6$)	182.39 ± 186.79	9.72 ± 3.97	−90 ± 9	668.84 ± 275.92	644.12 ± 252.80	1 ± 40
	Sand (2016–2017)					
Flood avg. ($n = 3$)	19.78 ± 5.01[a]	15.98 ± 6.71	−11 ± 16	124.74 ± 104.03	88.62 ± 31.25	6 ± 83
Control avg. (n = 2)	52.81 ± 4.01[ab]	9.25 ± 2.16[b]	−83 ± 3	1165.08 ± 781.98	354.45 ± 111.96	−65 ± 14
	Fine sandy loam (2015–2016)					
Flood avg. ($n = 3$)	13.98 ± 4.59	22.99 ± 20.04	56 ± 142	59.70 ± 36.88	114.98 ± 69.64	107 ± 113
Control avg. ($n = 6$)	12.02 ± 5.30[b]	32.39 ± 11.12[b]	209 ± 149	122.03 ± 70.66	118.11 ± 70.63	20 ± 79
	Fine sandy loam (2016–2017)					
Flood avg. ($n = 2$)	53.20 ± 49.06	65.24 ± 0.06	113 ± 197	233.70 ± 288.74	66.61 ± 1.99	23 ± 152
Control avg. ($n = 2$)	64.35 ± 8.96	49.96 ± 14.11	−23 ± 11	123.6 ± 5.54	316.59 ± 391.19	164 ± 329

[a]Significance of a two-sample *t* test comparing initial NO_3^-–N load between flood and control plots.
[b]Significant difference between the before and after NO_3^-–N load within a plot.

quantify NO_3^- leaching and major N transformation processes in the root zone induced by the application of large water amounts typical for Ag-MAR practices. Large soil columns (80 cm tall, 20 cm in diameter) were built from polyvinyl chloride (PVC) pipe (Figure 1). This column size was chosen to minimize sidewall flow (1:4 width/depth ratio) and to encompass some of the heterogeneity of the NO_3^- distribution observed within the field cores. The soils for the laboratory experiments were excavated in 10-cm intervals from the control treatment at both field sites in order to represent pre-flooding conditions. The columns were packed with the soil collected from the field sites in 10-cm intervals, to a depth of 80 cm and a measured average bulk density of 1.58 g cm^{-3} (sand) and 1.65 g cm^{-3} (fine sandy loam). Prior to and after completion of the flooding experiments, soil samples were taken at 10-cm intervals to constrain both the organic N and inorganic N pools within the soil matrix. Soil samples were analyzed in triplicate samples for NO_3^-–N, NH_4^+–N, and TN using the standard protocols as detailed above.

Each soil column was equipped with three volumetric soil water content (VWC) sensors at 5-, 35-, and 65-cm depth (Acclima TDR-310S), a dissolved O_2 sensor at 20-cm depth (PreSens, Fibox 4), and three discrete pore water sampling ports at 5-, 35-, and 65-cm depth (Soil Moisture, Model 190D4). The VWC was measured continuously at 1-min intervals. Discharge from the soil column was continuously measured in 5-min intervals using a tipping bucket rain gauge (Acurite, Model 00899). A vacuum of 50.80–67.73 mbar (1.5–2 inches Hg) was applied to the bottom of the soil columns in order to represent the matric potential and prevent the buildup of an artificial water table (Lewis & Sjöstrom, 2010). From the discharge, 50-ml water samples were collected at flow-dependent intervals ranging from 5 to 60 min and then analyzed for NO_3^-–N and NH_4^+–N.

Two flooding frequency treatments (low frequency [LF; flooding every 1–2 wk] and high frequency [HF; flooding every 72 h]) and two soil textures (sand [Delhi site] and fine sandy loam [Modesto site]) were tested with the soil column experiments for a total of four treatments. During each column experiment, three water applications (WAs), each of 15 cm, were made to each soil column (hereafter referred to as WA1, WA2, and WA3 respectively). Each 15 cm of water added represented 0.47 pore volumes of the 80-cm column for the sand, and 0.51 pore volumes for the fine sandy loam. The LF treatment was a true replicate of the water applications made at both field sites, consisting of three consecutive WAs in total with a 168-h (1-wk) break between WA1 and WA2, and a 336-h (2-wk) break between WA2 and WA3. In the HF treatment three WAs were made, each 72 h apart. An individual WA consisted of applying tap water (with nondetect concentrations of NO_3^-–N) equivalent to 15 cm of water depth over a period of 0.5 h onto the soil surface of the column using a perforated bucket to minimize erosion. Twenty-four hours before the start of the column experiments, the soil columns were brought up to the same VWC as was observed at each field site prior to the start of the Ag-MAR field experiments (sand: 0.1–0.15 cm^3 cm^{-3}; fine sandy loam: 0.2–0.25 cm^3 cm^{-3}), by applying a water application of ~8 cm such that soil volumetric water contents increased to between 0.1 and 0.2 cm^3 cm^{-3}.

2.2.2 | Soil incubations and NO_3^-–N mass balance calculations

Mineralization and denitrification incubations were performed on field soils in order to constrain transformation rates under ideal conditions. Net mineralization potential, the rate at which a soil converts organic N into inorganic N, was evaluated using methods outlined in Wade et al. (2018), where 10 g of soil from each 10-cm soil layer was air dried and sieved through a 2-mm sieve. Initial inorganic N levels were measured in each soil layer according to the methods described in Section 2.1.2 before samples were brought up to 55% water holding capacity, in order to maximize aerobic microbial activity (Linn & Doran, 1984), and incubated for 2 wk. Inorganic N levels were remeasured and mineralization rates were calculated as the difference in N concentrations between the initial and ending time of the experiment.

Denitrification incubations were measured according to the acetylene-inhibition method described in Smith et al. (1978), and gas samples were collected after 30 min, 90 min, and 1 d of incubation time. Samples were analyzed by gas chromatography for N_2O (Model GC-2014; Shimadzu Scientific Instruments).

In order to evaluate NO_3^- leaching potential (i.e., the potential for soil residual NO_3^- to be transported out of the soil profile), a NO_3^- mass balance for each soil column was calculated. Total mass of specific N species (NO_3^-–N, NH_4^+–N) in the soil (solid samples) was calculated as

$$M_{\text{soil}} = \sum_{i=1}^{n} C_n V_n \rho_n \quad (1)$$

where $M_{\text{soil}}$is the mass of the N species within the soil column (μg), n is the soil layer of the column (10-cm intervals to a depth of 80 cm), C is the concentration of the N species in the soil (μg g^{-1} soil), V is the volume of the soil layer (cm^3) and ρ is the density of the soil (g cm^{-3}). Mass loads of NO_3^- leaving the column as leachate (liquid samples) were calculated by

$$M_{\text{eff}} = \sum_{i=1}^{n} q_t C_t \Delta t \quad (2)$$

where M_{eff} is the mass of NO_3^-–N leaving the column during a flooding event, C_t is the concentration in an effluent sample (μg N ml^{-1}), q_t is the flow rate out of the column (ml min^{-1}) and Δt is the time step associated with C_t and q_t The mass balance for NO_3^- within the soil column is then represented by the typical mass balance equation:

$$I - O = \Delta S \quad (3)$$

where I represents the biogeochemical creation or addition of NO_3^- to the system, O represents the biogeochemical consumption or leaching of NO_3^- from the system, and ΔS represents the change of storage of NO_3^- mass within the system. When considering the NO_3^- mass balance, the only input considered in this mass balance is the creation of NO_3^- through mineralization and subsequent nitrification (conversion of organic N to NH_4^+, and conversion of NH_4^+ to NO_3^- measured in the soil profile). The water used for flooding contained negligible amounts of N species (<0.05 mg L^{-1} NO_3^-–N, NH_4^+–N). Outputs considered can include N transformations such as immobilization and denitrification, or physical processes such as NO_3^- leaching measured in the effluent (i.e., M_{eff}). Change in storage is represented by the difference between the before and after N profiles in the soil column experiments.

3 | RESULTS

3.1 | Field trials

The two almond orchards were flooded with 61–66.4 cm (about 2 ft) of water during the winters (December–January) of 2015–2016 and 2016–2017 (Supplemental Table S2). Soil moisture in the flood treatment for the sand reached saturation (0.4 cm^3 cm^{-3}) and returned back to pre-flooding soil water content (0.1–0.15 cm^3 cm^{-3}) within 12 h after Ag-MAR water application. Infiltration rates for the fine sandy loam were less rapid than for the sand, and an estimated 81–96% of the applied water for Ag-MAR left the root zone, depending on the year (Supplemental Table S3). Moisture sensors showed that flooding events on the fine sandy loam took between 48 and 72 h to return from saturation (0.35–0.4 cm^3 cm^{-3}) to pre-flooding soil water content (0.15–0.2 cm^3 cm^{-3}).

The data from the field experiments show large amounts of variance in NO_3^-, across both treatments and year. The NO_3^-–N load within the 400-cm soil cores taken from the sand site before the flooding events ranged between 68.0 and 570.1 kg ha^{-1} in the flood treatment and between 446.9 and 1,501.3 kg ha^{-1} in the control (plots only receiving winter precipitation) in 2015–2016. In 2016–2017, NO_3^-–N load ranged between 60.2 and 244.7 kg ha^{-1} in the flood treatment and between 612.1 and 1,718.0 kg ha^{-1} in the control (Table 1). Total NO_3^-–N loads in the 400-cm soil cores taken from the flood-irrigated fine sandy loam before Ag-MAR flooding were lower than those from the sand, between 26.0 and 99.1 kg ha^{-1} in the Ag-MAR treatment and 21.3 and 201.6 kg ha^{-1} in the control in 2015–2016. In 2016–2017, the observed range was between 29.5 and 437.9 kg ha^{-1} in the Ag-MAR treatment and between 119.7 and 127.5 kg ha^{-1} in the control (Table 1). Although the differences in the field data are mostly non-significant, there are general directional trends that can be identified.

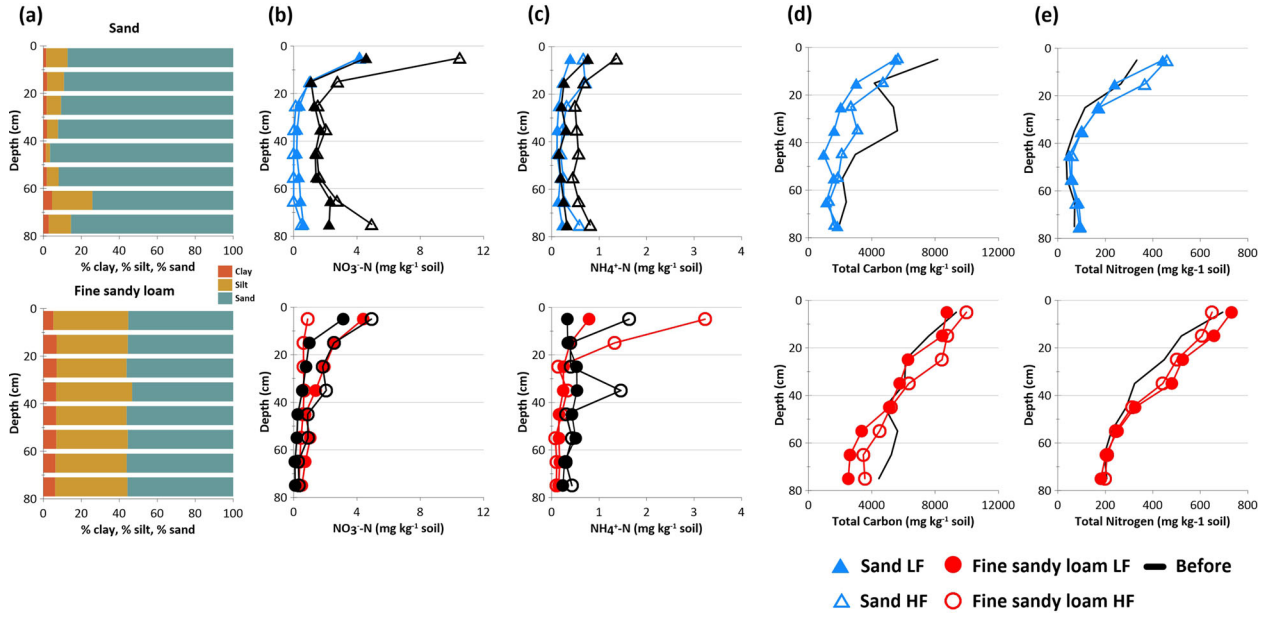

FIGURE 2 Initial characterization of field soils with depth for (a) texture, (b) NO_3^-–N, (c) NH_4^+–N, (d) total C (TC), and (e) total N (TN). LF, low frequency treatment (1–2 wk), HF, high frequency treatment (72 h)

The two sites exhibited opposing trends in the NO_3^- profiles resulting from the Ag-MAR flooding events in the 2015–2016 field experiments. The sand shows a general decrease in NO_3^-–N load in the soil profile after Ag-MAR flooding, whereas the fine sandy loam shows a general increase in NO_3^-–N load after flooding events. These trends are not as apparent in the 2016–2017 season, where the sand profile shows no strong directional shift following Ag-MAR flooding events, and the fine sandy loam shows only a slight increase in NO_3^-–N load after flooding (Table 1). The high variance of NO_3^-–N measured across the field sites results in a lack of significant conclusions that can be made regarding NO_3^-–N leaching due to Ag-MAR flooding events from the field data. Additionally, in the case of the fine sandy loam, where there is a net increase in NO_3^- between the before and after residual soil profile, an estimation of NO_3^- leached during Ag-MAR is not possible, highlighting the importance of controlled, high-resolution laboratory experiments.

3.2 | Soil column experiments

3.2.1 | Soil NO_3^-–N mass balance and transport

The initial soil NO_3^-–N and NH_4^+–N concentrations for the sand LF column ranged from 1.09 to 4.58 mg kg^{-1} for NO_3^-–N, and 0.15 to 0.76 mg kg^{-1} NH_4^+–N (Figure 2). The highest concentrations were located in the top 10 cm, whereas the lowest were found in the 30-to-50-cm range. The soil for the fine sandy loam LF column showed concentrations ranging from 0.09 to 3.12 mg kg^{-1} NO_3^-–N, and 0.237 to 0.531 mg kg^{-1} NH_4^+–N. Nitrate concentrations for the fine sandy loam decreased with increasing depth, whereas ammonium concentrations were greatest at 20-to-60-cm depth (Figure 2).

The initial soil NO_3^-–N and NH_4^+–N concentrations for sand HF ranged from 1.50 to 9.13 mg kg^{-1} NO_3^-–N, and 0.49 to 1.36 mg kg^{-1} NH_4^+–N. The fine sandy loam HF concentrations ranged from 0.29 to 4.91 mg kg^{-1} NO_3^-–N, and 0.29 to 2.20 mg kg^{-1} NH_4^+–N (Figure 3). This is an average total increase of 60 ± 28% for the sand and 127 ± 15.8% for the fine sandy loam in initial NO_3^- mass compared with the LF initial conditions in the soil profile before flooding.

The NO_3^- breakthrough curves of the fine sandy loam LF and HF column experiments were similar in shape, but the peak concentration reached during WA1 in the HF experiment was twice the peak concentration during the LF experiment (Figure 4c, d). Interestingly, the fine sandy loam LF experiment showed a distinct secondary peak during WA1 and WA2 around 30 h after water application. During the fine sandy loam HF experiment, the late secondary peak seen in the LF experiment (Figure 4c, d) was missing. Effluent concentrations in the fine sandy loam HF were much lower in WA2 and WA3, never exceeding 1 mg L^{-1} NO_3^-–N, with long periods of zero NO_3^-–N concentration.

Both of the sand LF and HF experiments showed narrow peaks in the NO_3^- breakthrough curve in WA1 with peak NO_3^-–N concentrations in the effluent of 18.4 and 26.72 mg L^{-1} during the sand LF and sand HF, respectively (Figure 4a, b). The sand HF did show the same shift in the NO_3^- peak as observed in sand LF WA2 and WA3, but the sand HF peaks

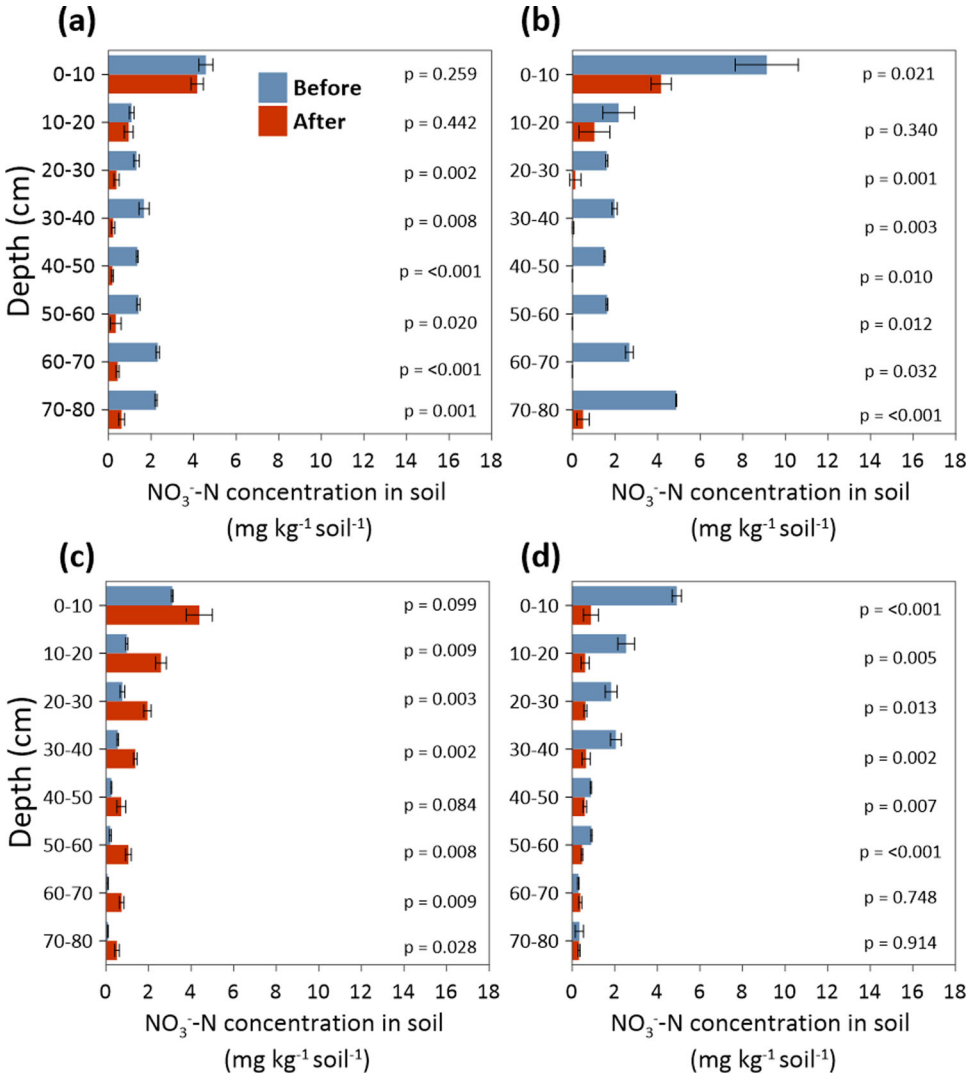

FIGURE 3 Comparison of before (blue bars) and after (red bars) NO_3^-–N loads in the soil profiles of the soil column experiments, (a) sand low-frequency treatment (LF), (b) sand high-frequency treatment (HF), (c) fine sandy loam LF, and (d) fine sandy loam HF. Error bars represent one standard deviation of NO_3^-–N in soil profile. *P* values represent the statistical significance that the before and after values measured in the respective soil layer are not equal

were of lower magnitude (LF WA2 and WA3 NO_3^-–N peaks were 7.58 and 9.27 mg L^{-1} compared with HF WA2 and WA3 NO_3^-–N peaks of 2.35 and 2.93 mg L^{-1}; Figure 4a, b).

The same directional trends in the residual soil NO_3^-–N of the 2015–2016 field experiments (Section 3.1) were observed in the corresponding LF soil column experiments (Figure 3). For the fine sandy loam, there was a greater amount of NO_3^-–N measured in the soil profile post-flooding than was initially present. In contrast, the sand profile showed a general decrease in NO_3^-–N measured in the soil profile post-flooding (Figure 3). However, effluent loads measured during the soil column experiments indicate that both sites were leaching discernible quantities of NO_3^- from the upper root zone (top 80 cm, Figure 4). Both soil textures leached over 100% of the initially present NO_3^--N during the LF soil column experiments (Figure 5).

The effluent mass balance of the fine sandy loam LF experiment showed that 145.7 ± 5.8% (47.1 mg NO_3^-–N) of the initially measured NO_3^- (32.4 mg NO_3^-–N) in the soil profile leached after three WAs (73.0, 45.2, and 27.5% leached during WA1, WA2, and WA3, respectively) (Figure 5a). The fine sandy loam HF effluent concentrations showed that the majority of the initially measured soil NO_3^- (73.5 mg NO_3^-–N) leached during WA1 (62.8% of the initial NO_3^- load), with only 1.0 and 0.9% leached during WA2 and WA3 (Figure 5b) for a total of 64.7 ± 10.4% (47.6 mg NO_3^-–N) (Figure 5b).

For the sand LF column experiment the total amount of NO_3^- leached was slightly lower than the fine sandy loam LF, with 137.3 ± 6.6% (112.4 mg NO_3^-–N) of the initially measured NO_3^- (81.9 mg NO_3^-–N) leached after three WAs (72.7, 25.5, and 39.2% leached during WA1, WA2, and WA3 respectively; Figure 5a). Overall, NO_3^- mass loss from the sand HF

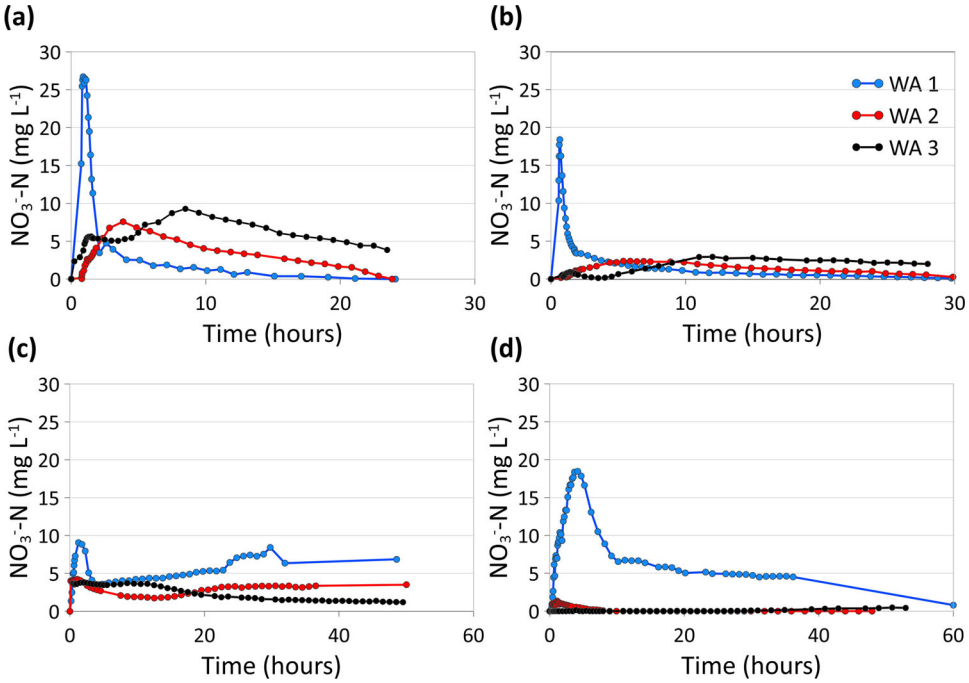

FIGURE 4 Observed NO_3^-–N concentrations in discharge through time, (a) sand low-frequency treatment (LF), (b) sand high-frequency treatment (HF), (c) fine sandy loam LF, and (d) fine sandy loam HF. WA, water application

column was lower than from sand LF. The percentage of NO_3^- leached from the initial sand HF profile (130.9 mg NO_3^-–N) during each WA was 24.5, 3.0, and 4.2% of the initial NO_3^- mass for a total of 31.7 ± 3.8% (41.6 mg NO_3^-–N) (Figure 5b).

3.2.2 | Mineralization incubations and NO_3^- mass balance

Both soil profiles showed similar mineralization rates, both in the maximum rate and in the depth distribution (Figure 6). The highest mineralization rates observed were 3.93 mg N kg^{-1} wk^{-1} (sand) and 3.41 mg N kg^{-1} wk^{-1} (fine sandy loam) in the top soil (0–10 cm), which decreased to 0.11 mg N kg^{-1} wk^{-1} (sand) and 0.08 mg N kg^{-1} wk^{-1} (fine sandy loam) at 50-to-70-cm depth. For the sand, the 50-to-70-cm depth showed indications of immobilization rather than mineralization, with a C/N ratio ranging from 53 to 61.

To account for the difference between the excess NO_3^- leached (137.3 ± 6.6% or 112.4 mg NO_3^-–N) during the sand LF column experiment and the change in residual NO_3^- left in the soil after flooding (a decrease of 43.8 mg NO_3^-–N), the mass balance required a mineralization contribution of 64.0 ± 8.2 mg N (Figure 7). The mineralization incubation assays for the sand determined a total mineralization potential of 103 mg N for the duration of the flooding experiment. The fine sandy loam LF mass balance required an even greater amount of 81.6 ± 10.9 mg N to explain the discrepancy between the 145.7 ± 5.8% (47.1 mg NO_3^-–N) of NO_3^- leached during the fine sandy loam LF experiment and the change in residual NO_3^- left in the soil after flooding (an increase of 34.5 mg NO_3^-–N) (Figure 7) . The total mineralization potential determined for the fine sandy loam from the assays was 133 mg N for the duration of the flooding experiment. When scaled for mineralization potential as a function of water content (Paul et al., 2003), the mineralization potential was 46.57 ± 14.29 and 68.55 ± 19.34 mg N for the sand and fine sandy loam. This indicates that the positive mass balance for both soil textures may be explained by mineralization processes (Figure 7). The HF experiments both showed a decrease in residual NO_3^- left in the soil after flooding. In general, they both have lower mineralization potential, and a higher denitrification potential, due to increased frequency of the water applications and higher water contents in the columns, conditions more conducive to denitrification (Butterbach-Bahl et al., 2013) (Figure 7).

4 | DISCUSSION

4.1 | Field scale residual NO_3^-–N profile trends

Wetting–drying cycles have been shown to affect microbial activity, and semiarid regions like California particularly exhibit pulses of increased microbial activity during

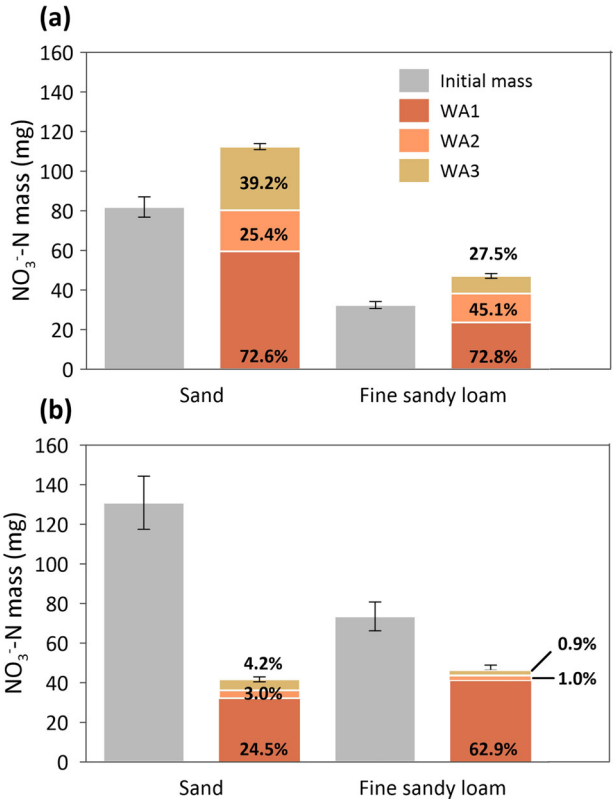

FIGURE 5 Initial soil NO_3^- mass and amount of NO_3^- leached during each water application (WA) during the (a) low frequency and (b) high frequency column experiments using sand and fine sandy loam soils. Percentages represent the percentage of initially present NO_3^-–N (gray bar) leached in each WA

significant precipitation events following long, dry periods (Austin et al., 2004; Noy-Meir, 1973). Our results indicate that the soil residual NO_3^- content after Ag-MAR can either increase or decrease in response to the pulsed water applications and related soil moisture-dependent N transformation processes. The 2015–2016 water year was ranked as a below average precipitation year in California and marked the final year of a 4-yr drought. In contrast, the 2016–2017 water year was the second wettest year in a 100-yr record (California Department of Water Resources, 2017). Thus, variation in precipitation between the 2015–2016 and 2016–2017 Ag-MAR field experiments may have distinctly affected biogeochemical processes and their potential rates and magnitudes at the field scale as indicated in Table 1. Although there is a lack of statistically significant trends between treatments and years in the field data, the finer texture soil (i.e., fine sandy loam) showed a clear increase in residual soil NO_3^- after flooding. Similar trends have been observed in previous studies by Chau et al. (2011) and Gregorich et al. (1991), who found greater amounts of mineralization and microbial activity in finer textured soils after irrigation or precipitation events. They concluded that the fine sandy loam in conjunction with a low K_{sat} of 3.3 mm h^{-1} in the deeper profile may create an environment where mineralization and nitrification processes are dominating over advective transport, resulting in a net increase of NO_3^- in the residual soil profile post-Ag-MAR. However, it is also important to note that in the flood treatment of the fine sandy loam residual NO_3^- increase was less than the increase observed in the control, indicating that the flood treatment likely experienced more NO_3^- leaching than the control. This is further supported by our soil column experiments, where the fine sandy loam LF shows a net increase in residual NO_3^- in the soil profile, but also a large amount of NO_3^- exported out of the column with the effluent.

4.2 | Biogeochemical processes under varying flooding frequencies

During the LF treatment, over 100% of the initially present NO_3^- was leached from the soil columns, indicating that organic N mineralization was occurring at significant rates in between flooding events. Under ideal conditions (i.e., 55% water holding capacity, ~0.16–0.25 cm^3 cm^{-3} depending on soil layer) both soils would have the potential to mineralize inorganic NO_3^- at a profile average rate of 7.0 mg N kg^{-1} wk^{-1} for the sand and 8.3 mg N kg^{-1} soil wk^{-1} for the fine sandy loam. Mineralization at these rates well exceed the amounts needed to explain the positive N mass balance observed in the column experiments. Moisture conditions for mineralization were near ideal 24–48 hours after each WA (e.g., water content ranged between 55 and 100% of water holding capacity, Supplemental Figure S3 and S4). Although 72.6 ± 4.3% (sand) and 72.8 ± 3.7% (fine sandy loam) of the initial soil NO_3^- was leached during WA1, we estimate that 46.6 ± 14.29 mg (sand) and 68.55 ± 19.34 mg (fine sandy loam) of new NO_3^- was mineralized between flooding events, which then became susceptible to leaching during subsequent WAs. This is further supported by the amounts of NO_3^- leached during LF WA2 and 3 (64.6 and 72.6% of initial soil NO_3^- for the sand and fine sandy loam, respectively), which combined with WA1 exceeded the initial soil NO_3^- amount by 30.5 (sand) and 14.7 mg (fine sandy loam), respectively.

When the timing between flooding events was decreased to 72 h (HF treatment), 24.5 ± 2.9% (sand) to 62.9 ± 5.6% (fine sandy loam) of the initial soil NO_3^- was leached during WA1, and markedly lower NO_3^- concentrations were observed in the effluent during WA2 and WA3 than during the LF experiment. The total amounts of NO_3^- leached during HF WA2 and WA3 only accounted for 6.7% (sand) and 1.9% (fine sandy loam) of the initially present NO_3^-, indicating lower contributions from mineralization, likely due to the shorter time periods between flooding events. This is further supported by the pore water NO_3^- data shown in Supplemental Figures S1 and S2. The sand HF experiment clearly lacks the increase in pore

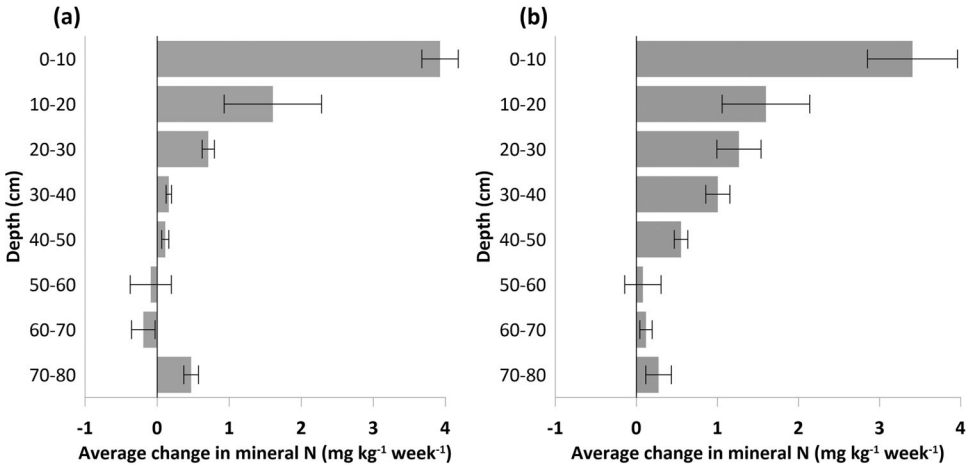

FIGURE 6 Mineralization rates for the (a) sand and (b) fine sandy loam

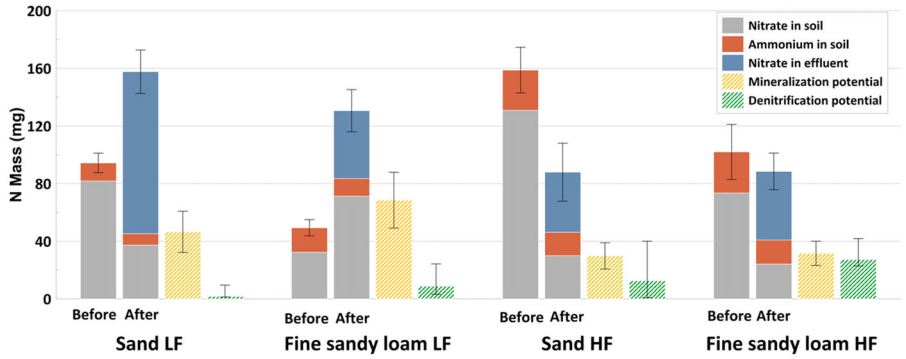

FIGURE 7 Total NO_3^- mass balance for soil columns. Error bars represent one standard deviation of the aggregated error for all components of a single column. LF, low-frequency treatment; HF, high-frequency treatment

water NO_3^- concentrations at the beginning of WA2 and WA3 that were observed during the LF experiment, indicating that a breakthrough of recently mobilized NO_3^- through the column was not occurring during the HF experiment. Similar patterns were observed for the HF experiment conducted with the fine sandy loam (Supplemental Figure S2). These dynamics support the hypothesis that less mineralization occurred in the shorter frequency (72-h) recharge experiment.

The NO_3^- mass balance of the HF experiments indicates that biogeochemical processes other than mineralization might have played a role. Although O_2 levels stayed well above 10% during the HF experiment (Supplemental Figures S3 and S4), the NO_3^- mass balance indicates that there likely was a significant amount of denitrification occurring, possibly restricted to microsites (i.e., saturated immobile pore space) of the soil profile that provided conditions supportive of denitrification (Groffman et al., 2009; Parkin, 1987). In addition, temporary microbial immobilization of inorganic N to organic N within the soil profile might have occurred (Johnsson et al., 1987, Paul & Clark, 2000, Romero et al., 2015). Based upon the denitrification incubations, and previous research concerning anaerobic microbial activity as a function of percent water filled pore space (Bateman & Baggs, 2005), the estimated denitrification potentials of the soil columns were 0.89–40.04 mg N (sand HF) and 22.83–41.91 mg N (fine sandy loam HF), respectively (Figure 7). Several layers in both soil textures had negative rates of net mineralization in the incubations (Figure 6), indicating that immobilization could also play a role in transforming inorganic N into organic N following WAs, which could act as a temporary sink of NO_3^- (Azam et al., 1988; Burger & Jackson, 2003; Recous et al., 1990).

The mineralization rates for the sand and fine sandy loam observed in this experiment are comparable with the rates found in other agricultural soils. Springob and Kirchmann (2003) found mineralization rates of 0.42–5.39 mg N kg^{-1} wk^{-1} in sandy and sandy loam soils in the top 28 cm, whereas Wade et al. (2016) found mineralization rates in the top 25 cm

of soil to be, on average, 1.61 mg N kg^{-1} wk^{-1}, which is comparable to our soils that mineralized 3.93 mg N kg^{-1} wk^{-1} (sand) and 3.41 mg N kg^{-1} wk^{-1} (fine sandy loam) in the top soil (0–10 cm) (Figure 6).

4.3 | Implications for field-scale NO_3^- leaching

The soil column Ag-MAR experiments allowed for a controlled setting to investigate N cycling and N transport processes at finer temporal and spatial scales than was possible in the field. The column experiments confirmed our hypothesis that both soil texture and the time interval between water applications influence NO_3^- leaching amounts. We found that irrespective of soil texture or treatment, most NO_3^- was leached during the first water application, transporting 50–97% of the total observed effluent NO_3^- mass out of the column. Although we conducted two sets of column experiments comparing two soil textures and flooding frequencies, the soil core data collected from the field sites highlight the huge variability in residual soil NO_3^- mass that can be observed just at the plot or field scale and the need for appropriate scaling techniques to reliably estimate NO_3^- leaching potential in agricultural soils subject to Ag-MAR at the field scale. Baram et al. (2016) showed that using the spatial average of all observed NO_3^- concentrations within a field can sufficiently capture the variability in N mass balance.

Our analysis showed that when scaled up to the field, the amount of NO_3^- leached from the soil columns in response to the 45 cm of applied water for the LF and HF experiments were 33.11 (0.72 kg ha^{-1} · cm H_2O) and 12.82 kg ha^{-1} (0.28 kg ha^{-1} · cm H_2O) NO_3^-–N for the sand, whereas the fine sandy loam LF and HF were 14.53 (0.32 kg ha^{-1} cm^{-1} H_2O) and 14.90 kg ha^{-1} (0.33 kg ha^{-1} cm^{-1} H_2O) NO_3^-–N, respectively. These amounts are comparable with a NO_3^- leaching study conducted by Onsoy et al. (2005) in a citrus orchard near Fresno, CA, where intensive irrigation of 174 cm yr^{-1} resulted in 93 and 275 kg ha^{-1} yr^{-1} NO_3^-–N leached from the 180-cm root zone, which translates to 0.53 and 1.58 kg ha^{-1} yr^{-1} NO_3^-–N cm^{-1} H_2O respectively, depending on fertilizer application rate (110–365 kg ha^{-1} yr^{-1} NO_3^-–N). Bachand et al. (2016) reported an estimated NO_3^-–N loss of 1.64 kg ha^{-1} cm^{-1} H_2O recharged on a mixture of sandy loam and loamy sand soils, growing alfalfa (*Medicago sativa* L.) and wine grapes, in California's Central Valley.

For our soil column experiments, NO_3^- leaching for the sand LF and HF was estimated at 0.72 and 0.28 kg ha^{-1} cm^{-1} H_2O respectively, and the fine sandy loam LF and HF to be 0.32 and 0.33 kg ha^{-1} cm^{-1} H_2O, respectively. The sand soil column estimates are similar to the average NO_3^- leaching amount of 0.77 kg ha^{-1} cm^{-1} H_2O we estimated for the 2016 field-collected soil cores. Our numbers are 30–50% of what Bachand et al. (2016) reported but are comparable with the NO_3^- leaching estimates Onsoy et al. (2005) estimated for the low fertilizer application rate treatment (110 kg ha^{-1} yr^{-1} NO_3^-–N). Comparison of our NO_3^- leaching amounts with Onsoy et al. (2005) highlights that the NO_3^- leaching amounts observed during our winter recharge event are comparable in magnitude with the amount of NO_3^- leached during the growing season in the citrus orchard near Fresno, CA. This opens the question whether the combination of winter Ag-MAR and growing season irrigation would effectively double the annual amount of NO_3^- leached from the root zone or whether the increase in soil NO_3^- due to mineralization after Ag-MAR events could potentially reduce fertilizer needs in subsequent growing seasons.

Some answers can be provided to this question based on our field and column experiments. First, it is important to note that in all soil column experiments, regardless of treatment or soil texture, the NO_3^- concentration of the total recharge was always below the USEPA maximum contaminant level of 10 mg NO_3^-–N L^{-1} (sand LF = 7.22 mg L^{-1}, sand HF = 2.81 mg L^{-1}, fine sandy loam LF = 3.18 mg L^{-1}, fine sandy loam HF = 3.26 mg L^{-1}). Additionally, the bulk of NO_3^- transport comes at the beginning of the water application, often within the first few hours in coarse-textured soils.

These dynamics have several implications both for the Ag-MAR best practices to minimize NO_3^- leaching, as well as growing season N management. Because the majority of the residual soil NO_3^- is leached at the beginning of Ag-MAR events, growing season nutrient needs need to be carefully managed on fields considered for winter Ag-MAR to reduce the residual NO_3^- content of the soil at the end of the growing season. Management practices that reduce the residual N at the end of a growing season (cover cropping, high nutrient use efficiency strategies, etc.) will be beneficial at Ag-MAR sites in decreasing the NO_3^- leaching potential from the root zone. At the same time, our results highlight that coarse-textured or high-K_{sat} soils promote fast and nearly complete (>70%) leaching of residual soil NO_3^- within hours of the first water application. Thus, it is unlikely that managing Ag-MAR systems for environmental conditions that promote denitrification, which often can be achieved by continuous flooding over several hours or days, will have much of an effect on reducing the leaching of NO_3^- already present in the soil at the beginning of the water application. However, prioritizing continuous flooding and decreasing the time between water applications will likely decrease the mineralization potential and thus decrease total leached NO_3^- amounts.

Although this research study highlighted the impact that the time interval between water applications may have on biogeochemical forcing, other Ag-MAR management variables exist that may influence NO_3^- leaching potential and site suitability for Ag-MAR projects. These include

physically manageable factors, such as flooding duration and timing within the season, and site-specific considerations, such as textural properties, hydrogeology, organic C/N pools, and the mineralization–denitrification potential of the site's soils. Future research should place emphasis on the development of models that can represent the biogeochemical processes observed under Ag-MAR more fully to evaluate best Ag-MAR practices (Waterhouse et al., 2021).

5 | CONCLUSIONS

The field and soil column experiments conducted in this study highlight the importance of biogeochemical processes when considering NO_3^- leaching potential during winter groundwater recharge on agricultural fields (Ag-MAR). With 137.3 ± 6.6% (sand) and 145.7 ± 5.8% (fine sandy loam) of the initially present NO_3^- leached during low-frequency (1-2 wk apart) flooding, our results show that using soil cores obtained in the field before and after winter recharge events to estimate NO_3^- leaching potential do not adequately capture total NO_3^- leaching amounts. This is because repeated, pulsed water applications for groundwater recharge, particularly if applied with long time intervals between events, provide environmental conditions promoting the mineralization of organic N to NO_3^-. Despite their contrasting soil texture, both soils studied here were capable of mineralizing organic N at a profile-average rate of 7.0–8.3 mg N kg^{-1} wk^{-1}. Comparison of different flooding frequencies (e.g. 72-h vs 1-wk time intervals between flooding events) showed that longer time intervals resulted in increased N mineralization potential, and consequently higher amounts of NO_3^- leached during subsequent flooding events. The column experiments further showed that the majority of the total NO_3^- leached over the course of the groundwater recharge event was leached during the first few hours of the first water application when environmental conditions were unfavorable for denitrification (such as anoxic conditions), a process that reduces NO_3^- to different gaseous N_2O products.

Our results helped identify and quantify important biogeochemical processes that need to be considered when assessing the environmental tradeoffs of practicing Ag-MAR on agricultural fields in production. Specifically, our results indicate that winter flooding on agricultural fields for groundwater recharge produces environmental conditions that promote N transformation processes that can produce more residual soil NO_3^-. However, more research is needed comparing different soil textures and Ag-MAR practices to fully understand the impact of winter recharge (amounts, timing, flooding duration) on the organic C/N pools and N cycling processes, including NO_3^- leaching and mineralization–denitrification potential. Simulating these biogeochemical processes with reactive transport instead of conservative transport models should allow improving estimates of total NO_3^- leaching amounts during Ag-MAR, which can guide Ag-MAR best practice development.

ACKNOWLEDGMENTS

This research was supported by funding from the Almond Board of California and the Bureau of Reclamation (Grant R16PC00029). The authors would like to thank Seanna McLaughlin, Cristina Prieto Garcia, Roger Duncan, and David Doll for their help with the field and laboratory experiments. This project was also supported by the USDA National Institute of Food and Agriculture, Hatch Project no. CA-D-LAW-2513-H.

AUTHOR CONTRIBUTIONS

Nicholas Paul Murphy: Conceptualization; Data curation; Formal analysis; Investigation; Methodology; Project administration; Resources; Validation; Visualization; Writing-original draft; Writing-review & editing. Hannah Waterhouse: Conceptualization; Investigation; Resources; Writing-review & editing. Helen E. Dahlke: Conceptualization; Funding acquisition; Investigation; Methodology; Project administration; Resources; Supervision; Visualization; Writing-review & editing.

CONFLICT OF INTEREST

The authors declare no conflict of interest.

DATA AVAILABILITY STATEMENT

Raw data are available from the corresponding author upon request for both field and laboratory experiments. Data include soil, pore water, and effluent analysis for field and laboratory experiments outlined in Section 2, soil column NO_3^-–N leaching mass balance calculations, mineralization potential and the conditional analysis based on water content, estimated deep percolation calculations, and soil column instrumentation data (VWC, dissolved O_2).

ORCID

Nicholas P. Murphy https://orcid.org/0000-0001-8442-0747

Hannah Waterhouse https://orcid.org/0000-0002-8387-4453

Helen E. Dahlke https://orcid.org/0000-0001-8757-6982

REFERENCES

Abiye, T. A., Sulieman, H., & Ayalew, M. (2009). Use of treated wastewater for managed aquifer recharge in highly populated urban centers: A case study in Addis Ababa, Ethiopia. *Environmental geology*, *58*, 55–59. https://doi.org/10.1007/s00254-008-1490-y

Aronsson, P. G., & Bergström, L. F. (2001). Nitrate leaching from lysimeter-grown short-rotation willow coppice in relation to N-application, irrigation and soil type. *Biomass and Bioenergy*, *21*, 155–164. https://doi.org/10.1016/S0961-9534(01)00022-8

Austin, A. T., Yahdjian, L., Stark, J. M., Belnap, J., Porporato, A., Norton, U., Ravetta, D. A., & Schaeffer, S. M. (2004). Water pulses and biogeochemical cycles in arid and semiarid ecosystems. *Oecologia*, *141*, 221–235. https://doi.org/10.1007/s00442-004-1519-1

Azam, F., Mahmood, T., & Malik, K. A. (1988). Inmobilization-remineralization of NO_3-N and total N balance during the decomposition of glucose, sucrose and cellulose in soil incubated at different moisture regimes. *Plant and Soil*, *107*, 159–163. https://doi.org/10.1007/BF02370542

Bachand, P. A., Roy, S. B., Choperena, J., Cameron, D., & Horwath, W. R. (2014). Implications of using on-farm flood flow capture to recharge groundwater and mitigate flood risks along the Kings River, CA. *Environmental science & technology*, *48*, 13601–13609.

Bachand, P. A. M., Roy, S., Stern, N., Choperena, J., Cameron, D., & Horwath, W. (2016). On-farm flood capture could reduce groundwater overdraft in Kings River basin. *California Agriculture*, *70*, 200–207. https://doi.org/10.3733/ca.2016a0018

Baram, S., Couvreur, V., Harter, T., Read, M., Brown, P. H., Hopmans, J. W., & Smart, D. R. (2016). Assessment of orchard N losses to groundwater with a vadose zone monitoring network. *Agricultural Water Management*, *172*, 83–95. https://doi.org/10.1016/j.agwat.2016.04.012

Bateman, E. J., & Baggs, E. M. (2005). Contributions of nitrification and denitrification to N_2O emissions from soils at different water-filled pore space. *Biology and fertility of soils*, *41*, 379–388. https://doi.org/10.1007/s00374-005-0858-3

Ben Moshe, S., Weisbrod, N., Barquero, F., Sallwey, J., Orgad, O., & Furman, A. (2020). On the role of operational dynamics in biogeochemical efficiency of a soil aquifer treatment system. *Hydrology and Earth System Sciences*, *24*, 417–426. https://doi.org/10.5194/hess-24-417-2020

Bergström, L., & Johansson, R. (1991). Leaching of nitrate from monolith lysimeters of different types of agricultural soils. *Journal of Environmental Quality*, *20*, 801–807. https://doi.org/10.2134/jeq1991.00472425002000040015x

Botros, F. E., Onsoy, Y. S., Ginn, T. R., & Harter, T. (2012). Richards equation-based modeling to estimate flow and nitrate transport in a deep alluvial vadose zone. *Vadose Zone Journal*, *11*(4). https://doi.org/10.2136/vzj2011.0145

Burger, M., & Jackson, L. E. (2003). Microbial immobilization of ammonium and nitrate in relation to ammonification and nitrification rates in organic and conventional cropping systems. *Soil Biology and Biochemistry*, *35*, 29–36. https://doi.org/10.1016/S0038-0717(02)00233-X

Butterbach-Bahl, K., Baggs, E. M., Dannenmann, M., Kiese, R., & Zechmeister-Boltenstem, S. (2013). Nitrous oxide emissions from soils: How well do we understand the processes and their controls? *Philosophical Transactions of the Royal Society B*, *368*(1621). https://doi.org/10.1098/rstb.2013.0122

Cabrera, M. L. (1993). Modeling the flush of nitrogen mineralization caused by drying and rewetting soils. *Soil Science Society of America Journal*, *57*, 63–66. https://doi.org/10.2136/sssaj1993.03615995005700010012x

California Department of Water Resources. (2017). *Water year 2017: What a difference a year makes*. California Department of Water Resources.

Cambardella, C. A., Moorman, T. B., Jaynes, D. B., Hatfield, J. L., Parkin, T. B., Simpkins, W. W., & Karlen, D. L. (1999). Water quality in Walnut Creek watershed: Nitrate-nitrogen in soils, subsurface drainage water, and shallow groundwater. *Journal of Environmental Quality*, *28*, 25–34. https://doi.org/10.2134/jeq1999.00472425002800010003x

Chau, J. F., Bagtzoglou, A. C., & Willig, M. R. (2011). The effect of soil texture on richness and diversity of bacterial communities. *Environmental Forensics*, *12*, 333–341. https://doi.org/10.1080/15275922.2011.622348

Dahlke, H., Brown, A., Orloff, S., Putnam, D., & O'Geen, T. (2018). Managed winter flooding of alfalfa recharges groundwater with minimal crop damage. *California Agriculture*, *72*, 65–75. https://doi.org/10.3733/ca.2018a0001

Dalin, C., Taniguchi, M., & Green, T. R. (2019). Unsustainable groundwater use for global food production and related international trade. *Global Sustainability*, *2*. https://doi.org/10.1017/sus.2019.7

Di, H. J., & Cameron, K. C. (2002a). Nitrate leaching and pasture production from different nitrogen sources on a shallow stoney soil under flood-irrigated dairy pasture. *Soil Research*, *40*, 317–334. https://doi.org/10.1071/SR01015

Di, H. J., & Cameron, K. C. (2002b). Nitrate leaching in temperate agroecosystems: Sources, factors and mitigating strategies. *Nutrient cycling in agroecosystems*, *64*, 237–256. https://doi.org/10.1023/A:1021471531188

Dillon, P. J., Pavelic, P., Page, D., Beringen, H., & Ward, J. (2009). *Managed aquifer recharge: An introduction* (Waterlines Report Series 13). National Water Commission.

Doane, T. A., & Horwáth, W. R. (2003). Spectrophotometric determination of nitrate with a single reagent. *Analytical letters*, *36*, 2713–2722. https://doi.org/10.1081/AL-120024647

Forster, J. C. (1995). Soil physical analysis. In K. Alef & P. Nannipieri (Eds.), *Methods in soil microbiology and biochemistry* (pp. 105–121). Academic Press

Gaines, T. P., & Gaines, S. T. (1994). Soil texture effect on nitrate leaching in soil percolates. *Communications in Soil Science and Plant Analysis*, *25*, 2561–2570. https://doi.org/10.1080/00103629409369207

Gheysari, M., Mirlatifi, S. M., Homaee, M., Asadi, M. E., & Hoogenboom, G. (2009). Nitrate leaching in a silage maize field under different irrigation and nitrogen fertilizer rates. *Agricultural Water Management*, *96*, 946–954. https://doi.org/10.1016/j.agwat.2009.01.005

Goren, O., Burg, A., Gavrieli, I., Negev, I., Guttman, J., Kraitzer, T., & Lazar, B. (2014). Biogeochemical processes in infiltration basins and their impact on the recharging effluent, the soil aquifer treatment (SAT) system of the Shafdan plant, Israel. *Applied Geochemistry*, *48*, 58–69. https://doi.org/10.1016/j.apgeochem.2014.06.017

Gorski, G., Fisher, A. T., Beganskas, S., Weir, W. B., Redford, K., Schmidt, C., & Saltikov, C. (2019). Field and Laboratory Studies Linking Hydrologic, Geochemical, and Microbiological Processes and Enhanced Denitrification during Infiltration for Managed Recharge. *Environmental Science & Technology*, *53*, 9491–9501.

Gregorich, E. G., Voroney, R. P., & Kachanoski, R. G. (1991). Turnover of carbon through the microbial biomass in soils with different texture. *Soil Biology and Biochemistry*, *23*, 799–805. https://doi.org/10.1016/0038-0717(91)90152-A

Groffman, P. M., Butterbach-Bahl, K., Fulweiler, R. W., Gold, A. J., Morse, J. L., Stander, E. K., & Vidon, P. (2009). Challenges to incorporating spatially and temporally explicit phenomena (hotspots and hot moments) in denitrification models. *Biogeochemistry*, *93*, 49–77. https://doi.org/10.1007/s10533-008-9277-5

Harter, T., Onsoy, Y., Heeren, K., Denton, M., Weissmann, G., Hopmans, J., & Horwath, W. (2005). Deep vadose zone hydrology demonstrates fate of nitrate in eastern San Joaquin Valley. *California Agriculture*, *59*, 124–132. https://doi.org/10.3733/ca.v059n02p124

Johnsson, H., Bergstrom, L., Jansson, P. E., & Paustian, K. (1987). Simulated nitrogen dynamics and losses in a layered agricultural soil. *Agriculture, Ecosystems & Environment*, *18*, 333–356.

Kaiser, E. A., Mueller, T., Joergensen, R. G., Insam, H., & Heinemeyer, O. (1992). Evaluation of methods to estimate the soil microbial biomass and the relationship with soil texture and organic matter. *Soil Biology and Biochemistry*, *24*, 675–683. https://doi.org/10.1016/0038-0717(92)90046-Z

Kocis, T. N., & Dahlke, H. E. (2017). Availability of high-magnitude streamflow for groundwater banking in the Central Valley, California. *Environmental Research Letters*, *12*, 084009. https://doi.org/10.1088/1748-9326/aa7b1b

Lewis, J., & Sjöstrom, J. (2010). Optimizing the experimental design of soil columns in saturated and unsaturated transport experiments. *Journal of Contaminant Hydrology*, *115*(1–4). https://doi.org/10.1016/j.jconhyd.2010.04.001

Linn, D. M., & Doran, J. W. (1984). Effect of water-filled pore space on carbon dioxide and nitrous oxide production in tilled and nontilled soils. *Soil Science Society of America Journal*, *48*, 1267–1272. https://doi.org/10.2136/sssaj1984.03615995004800060013x

Lv, H., Lin, S., Wang, Y., Lian, X., Zhao, Y., Li, Y., Du, J., Wang, Z., Wang, J., & Butterbach-Bahl, K. (2019). Drip fertigation significantly reduces nitrogen leaching in solar greenhouse vegetable production system. *Environmental Pollution*, *245*, 694–701. https://doi.org/10.1016/j.envpol.2018.11.042

Miller, J. H., Ela, W. P., Lansey, K. E., Chipello, P. L., & Arnold, R. G. (2006). Nitrogen transformations during soil–aquifer treatment of wastewater effluent: Oxygen effects in field studies. *Journal of Environmental Engineering*, *132*, 1298–1306. https://doi.org/10.1061/(ASCE)0733-9372(2006)132:10(1298)

Noy-Meir, I. (1973). Desert ecosystems: Environment and producers. *Annual Review of Ecology and Systematics*, *4*, 25–51. https://doi.org/10.1146/annurev.es.04.110173.000325

O'Geen, A. T., Saal, M., Dahlke, H., Doll, D., Elkins, R., Fulton, A., Fogg, G., Harter, T., Hopmans, J. W., Ingels, C., Niederholzer, F., Solis, S. S., Verdegaal, P., & Walkinshaw, M. (2015). Soil suitability index identifies potential areas for groundwater banking on agricultural lands. *California Agriculture*, *69*, 75–84. https://doi.org/10.3733/ca.v069n02p75

Onsoy, Y. S., Harter, T., Ginn, T. R., & Horwath, W. R. (2005). Spatial variability and transport of nitrate in a deep alluvial vadose zone. *Vadose Zone Journal*, *4*, 41–54. https://doi.org/10.2113/4.1.41

Parkin, T. B. (1987). Soil microsites as a source of denitrification variability. *Soil Science Society of America Journal*, *51*, 1194–1199. https://doi.org/10.2136/sssaj1987.03615995005100050019x

Paul, E. A., & Clark, F. E. (2000). *Soil microbiology and biochemistry*. Academic Press.

Paul, K. I., Polglase, P. J., O'connell, A. M., Carlyle, J. C., Smethurst, P. J., & Khanna, P. K. (2003). Defining the relation between soil water content and net nitrogen mineralization. *European Journal of Soil Science*, *54*, 39–48. https://doi.org/10.1046/j.1365-2389.2003.00502.x

Phogat, V., Skewes, M. A., Cox, J. W., Sanderson, G., Alam, J., & Šimůnek, J. (2014). Seasonal simulation of water, salinity and nitrate dynamics under drip irrigated mandarin (*Citrus reticulata*) and assessing management options for drainage and nitrate leaching. *Journal of Hydrology*, *513*, 504–516. https://doi.org/10.1016/j.jhydrol.2014.04.008

Quanrud, D. M., Arnold, R. G., Wilson, L. G., Gordon, H. J., Graham, D. W., & Amy, G. L. (1996). Fate of organics during column studies of soil aquifer treatment. *Journal of Environmental Engineering*, *122*, 314–321. https://doi.org/10.1061/(ASCE)0733-9372(1996)122:4(314)

Recous, S., Mary, B., & Faurie, G. (1990). Microbial immobilization of ammonium and nitrate in cultivated soils. *Soil Biology and Biochemistry*, *22*, 913–922. https://doi.org/10.1016/0038-0717(90)90129-N

Romero, C. M., Engel, R., Chen, C., & Wallander, R. (2015). Microbial immobilization of nitrogen-15 labelled ammonium and nitrate in an agricultural soil. *Soil Science Society of America Journal*, *79*, 595–602. https://doi.org/10.2136/sssaj2014.08.0332

Schmidt, C. M., Fisher, A. T., Racz, A. J., Lockwood, B. S., & Huertos, M. L. (2011). Linking denitrification and infiltration rates during managed groundwater recharge. *Environmental Science & Technology*, *45*, 9634–9640.

Smith, M. S., Firestone, M. K., & Tiedje, J. M. (1978). The acetylene inhibition method for short-term measurement of soil denitrification and its evaluation using nitrogen-13. *Soil Science Society of America Journal*, *42*, 611–615. https://doi.org/10.2136/sssaj1978.03615995004200040015x

Sogbedji, J. M., van Es, H. M., Yang, C. L., Geohring, L. D., & Magdoff, F. R. (2000). Nitrate leaching and nitrogen budget as affected by maize nitrogen rate and soil type. *Journal of Environmental Quality*, *29*, 1813–1820. https://doi.org/10.2134/jeq2000.00472425002900060011x

Springob, G., & Kirchmann, H. (2003). Bulk soil C to N ratio as a simple measure of net N mineralization from stabilized soil organic matter in sandy arable soils. *Soil Biology and Biochemistry*, *35*, 629–632. https://doi.org/10.1016/S0038-0717(03)00052-X

Verdouw, H., Van Echteld, C. J. A., & Dekkers, E. M. J. (1978). Ammonia determination based on indophenol formation with sodium salicylate. *Water Research*, *12*, 399–402. https://doi.org/10.1016/0043-1354(78)90107-0

Wada, Y., Wisser, D., & Bierkens, M. F. (2014). Global modeling of withdrawal, allocation and consumptive use of surface water and groundwater resources. *Earth System Dynamics*, *5*, 15–40. https://doi.org/10.5194/esd-5-15-2014

Waddell, J. T., Gupta, S. C., Moncrief, J. F., Rosen, C. J., & Steele, D. D. (2000). Irrigation-and nitrogen-management impacts on nitrate leaching under potato. *Journal of Environmental Quality*, *29*, 251–261. https://doi.org/10.2134/jeq2000.00472425002900010032x

Wade, J., Horwath, W. R., & Burger, M. B. (2016). Integrating soil biological and chemical indices to predict net nitrogen mineralization across California agricultural systems. *Soil Science Society of America Journal*, *80*, 1675–1687. https://doi.org/10.2136/sssaj2016.07.0228

Wade, J., Waterhouse, H., Roche, L. M., & Horwath, W. R. (2018). Structural equation modeling reveals iron (hydr) oxides as a strong mediator of N mineralization in California agricultural soils. *Geoderma*, *315*, 120–129. https://doi.org/10.1016/j.geoderma.2017.11.039

Wang, H., Ju, X., Wei, Y., Li, B., Zhao, L., & Hu, K. (2010). Simulation of bromide and nitrate leaching under heavy rainfall and high-intensity irrigation rates in North China Plain. *Agricultural Water Management*, *97*), 1646–1654. https://doi.org/10.1016/j.agwat.2010.05.022

Waterhouse, H., Arora, B., Spycher, N. F., Nico, P. S., Ulrich, C., Dahlke, H. E., & Horwath, W. R. (2021). Influence of agricultural managed aquifer recharge (AgMAR) and stratigraphic heterogeneities on nitrate reduction in the deep subsurface. *Water Resources Research*, *57*, e2020WR029148. https://doi.org/10.1029/2020WR029148

Waterhouse, H., Bachand, S., Mountjoy, D., Choperena, J., Bachand, P., Dahlke, H., & Horwath, W. (2020). Agricultural managed aquifer recharge: Water quality factors to consider. *California Agriculture*, *74*, 144–154.

Zhou, J., Gu, B., Schlesinger, W. H., & Ju, X. (2016). Significant accumulation of nitrate in Chinese semi-humid croplands. *Scientific Reports*, *6*, 1–8.

SUPPORTING INFORMATION

Additional supporting information may be found online in the Supporting Information section at the end of the article.

How to cite this article: Murphy, N. P., Waterhouse, H., & Dahlke, H. E. Influence of agricultural managed aquifer recharge on nitrate transport: The role of soil texture and flooding frequency. *Vadose Zone J.* 2021;e20150. https://doi.org/10.1002/vzj2.20150